Dendritic growth velocities in an undercooled melt of pure nickel under static magnetic fields: a test of theory with convection

Jianrong Gao[a,*], Mengkun Han[a], Andrew Kao[b], Koulis Pericleous[b], Dmitri V. Alexandrov[c], Peter K. Galenko[d]

[a]Key Laboratory of Electromagnetic Processing of Materials (Ministry of Education), Northeastern University, Shenyang 110819, People's Republic of China

[b]Center for Numerical Modeling and Process Analysis, University of Greenwich, London SE10 9LS, United Kingdom

[c]Department of Mathematical Physics, Ural Federal University, 620000 Ekaterinburg, Russian Federation

[d]Department of Physics and Astronomy, Friedrich Schiller University of Jena, 07743 Jena, Germany

Abstract

Dendritic growth velocities in an undercooled melt of pure nickel under static magnetic fields up to 6 T were measured using a high-speed camera. The growth velocities for undercoolings below 120 K are depressed under low magnetic fields, but are recovered progressively under high magnetic fields. This retrograde behavior arises from two competing kinds of magnetohydrodynamics in the melt and becomes indistinguishable for higher undercoolings. The measured data is used for testing of a recent theory of dendritic growth with convection. A reasonable agreement is attained by assuming magnetic field-dependent flow velocities. As is shown, the theory can

also account for previous data of dendritic growth kinetics in pure succinonitrile under normal gravity and microgravity conditions. These tests demonstrate the efficiency of the theory which provides a realistic description of dendritic growth kinetics of pure substances with convection.

Keywords: Dendritic Solidification; Growth kinetics; Undercooling; Static magnetic field; Theory

---

* Corresponding author. Tel.: +86-24-83681915; fax: +86-24-83681758; e-mail address: jgao@mail.neu.edu.cn.

1. Introduction

Dendritic growth of crystals occurs in nature and metallurgy. Many studies were devoted to an understanding of the growth kinetics and pattern selection issues of this process. A number of theories were proposed and compared with experimental observations. The currently accepted theories [1, 2] include Ivantsovôs solution to the heat and mass transport issue at a needle-like dendritic tip and a microsolvability analysis for unambiguous selection of a tip radius at a given undercooling in terms of the anisotropy of crystal-melt interfacial energy. A third accepted theory is a linear approximation of non-equilibrium thermodynamics which becomes evident at high undercoolings and depends on the anisotropy of interface attachment kinetics [3]. Such theories are often combined and referred to as an assembled theory in literature. The LKT/BCT theory [4−6] is one such example and represents a full combination of the three theories. Although some studies concluded a general agreement between the LKT/BCT theory and experiment [7−9], a discrepancy remains in the low undercooling region. The measured dendritic growth velocities in pure substances were found to deviate from the predictions of the LKT/BCT theory significantly [10]. This is also true for dendritic tip radii measured in a transparent substance [11]. A microgravity experiment [12, 13] and phase field modeling [14−17] suggested that the discrepancy is likely to arise from an interaction of dendritic growth with fluid flow in an undercooled bulk melt. Thus, theoretical efforts have been made to bridge this discrepancy by the introduction of a rigorous treatment of the fluid flow effect on dendritic growth.

An early attempt was made by Boussiou and Pelce [18]. They extended Ivantsovôs theory by applying the Navier-Stokes equation to a tilted flow in a pure substance. They proposed a solution to the flow-modified heat transport issue in two-dimensional dendritic growth. They also worked out the microsolvability condition at low growth Peclet numbers and presented a selection criterion for the dendritic tip that relies on the anisotropy of the crystal-melt interfacial energy and on a longitudinal component of the tilted flow as well. Recently, Alexandrov and Galenko [19] extended this treatment to the dendrite tip growing at arbitrary growth Peclet numbers in a pure substance or a dilute alloy system. The selection criterion for the dendritic tip is dependent on the growth Peclet number. On the basis of this advancement, they proposed a combined three-dimensional theory for dendritic growth with convection [20]. For convenience, this new theory is termed as the Alexandrov-Galenko theory (AG theory for short). A preliminary test of the AG theory has already been conducted using a two-dimensional formalism [20]. It was shown that the AG theory can provide a satisfactory explanation of the dendritic growth velocities observed in containerlessly undercooled intermetallic compounds in the presence of a convective flow in a bulk volume [20, 21]. However, phase field modeling suggested that the influence of melt convection on a three-dimensional tip is more pronounced than on a two-dimensional tip [17, 22]. Thus, it is of great interest to perform a test of the three-dimensional AG theory using data measured under conditions of controllable melt convection.

In this paper, we report measurements of dendritic growth velocities of pure nickel

under static magnetic fields for a test of the three-dimensional AG theory [20]. The utilization of the static magnetic fields allowed us to tune forced convection in an undercooled melt continuously, thus providing much freedom for the test. Then we present a complementary test of the AG theory using literature data of dendritic growth velocities and dendritic tip radii of pure succinonitrile measured under normal gravity and microgravity conditions [13]. Finally, we compare the AG theory with phase field modeling of dendritic growth at high growth Peclet numbers [23].

2. Experimental details

The measurements were performed on a single glass-fluxed sample of pure nickel. The sample had a purity of 99.99% and a mass of about 1 g. A radio-frequency induction furnace was combined with a superconducting magnet to melt and solidify the sample under static magnetic fields up to B = 6 T. The sample was supported by a pan-like ceramic holder containing a small amount of soda lime glass, and was fixed between two opposite windings of a heating coil of the furnace. The vacuum chamber of the furnace was pumped to a vacuum pressure of 5.7×10^{-3} Pa and was backfilled with argon of 99.999% purity to a pressure of 5×10^{4} Pa. The sample was inductively heated, melted, and overheated under the protection of the argon atmosphere. Then, the heating power to the coil was reduced to about 14 % of the initial power. The sample was cooled and solidified spontaneously. In solidification, crystal nucleation occurred preferentially on the lower surface of the sample, which was in intimate contact with the fluxed glass. A recalescence process followed due to instantaneously

released latent heat. Under each of the static magnetic fields ranging between B = 0 T and B = 6 T, the melting-solidification cycle was repeated 20 to 30 times to produce a wide spectrum of undercooling. The surface temperature of the sample was measured using a single-color pyrometer with an accuracy of $\pm$ 6 K at a sampling rate of 100 Hz. Meanwhile, the recalescence process was monitored using a high-speed video camera at a frame rate of 87,600 fps. The video images were analyzed using an executable program running in the environment of the commercial software Matlab to determine the speed of an advancing recalescence front. The recalescence front was assumed to travel like a spherical wave starting from the nucleation site and advancing towards the other side of the sample surface at a constant speed. With the aid of the program, the location of the nucleation site on the sample surface was determined first. Then, the traveling distance of the recalescence front away from the nucleation site was determined as a function of time by analyzing the traces of the recalescence front. A linear law was fitted to the distance versus time relationship, and the slope of the linear law was taken as the traveling speed of the recalescence front. The speed of the recalescence event gave a good approximation of dendritic growth velocities in the undercooled sample due to a thermal diffusion distance shorter than a one-dimensional resolution of 100 μm of each pixel of the video images. The algorithm used in the program was exactly the same as that established by Binder using a free software, POV Ray 3.6, for the same purpose [24] but with an improved efficiency in determining the speed.

3. Results and discussion

3.1 Dendritic growth velocities of pure nickel under forced convection conditions

The measured dendritic growth velocities are plotted in Fig. 1 as a function of undercooling, ΔT. A power law is observed over a wide range of undercooling for each static magnetic field. The growth kinetics appears to be decelerated abruptly at a critical undercooling of ΔT_{crit} = 165 K, as evidenced by a negative deviation from the power law[1]. Such observations are in good agreement with the latest measurements on electromagnetically levitated nickel samples of higher purity [10]. However, there are distinct differences in the magnitude of the measured dendritic growth velocities. As displayed in Fig. 1, the present data for undercoolings below ΔT_{crit} shows a positive or a negative deviation depending on the static magnetic fields. These deviations are related to forced convection in the undercooled sample as explained below. Another deviation is observed for undercoolings above ΔT_{crit}. It is negative and independent of the magnetic fields. It is assumed to arise from the higher impurity concentration of the present sample because a reduced deviation was observed by one of the present authors using a purer material [28].

Forced convection is very common in inductively heated metallic melts and is active in the present sample. Unlike the electromagnetically levitated samples, the present sample was fixed on the sample holder. The forced convection inside it was expected to be weaker than in the electromagnetically levitated samples as suggested

[1] A similar deviation of dendritic growth kinetics from a power law was also observed for dilute Ni-B and Cu-O alloys [25,26] and can be interpreted by considering local non-equilibrium at a rapidly advancing crystal/liquid interface [27].

by Mullis et al. [26]. But, as seen in Fig. 1, the present data measured with no static magnetic fields shows higher growth velocities for undercoolings below 60 K than those measured in the electromagnetically levitated samples. This difference in the growth velocities seems to suggest stronger forced convection in the present sample. However, it can also be related to the tiny amount of the impurity in the present sample, which can promote dendritic growth at low undercoolings [10]. More studies need to be performed to clarify the reason for it. Here we focus our attention onto the effect of the static magnetic fields. As is shown elsewhere [29], forced convection in the electromagnetically levitated samples can be damped effectively by imposing a static magnetic field of 0.5 T or above. This damping is expected to be also effective on forced convection in the present sample. In order to prove this assumption, we modeled forced convection in a molten sample with a spherical geometry under a static magnetic field of B = 6 T numerically. As illustrated in Fig. 2, a maximum flow velocity of 0.0075 m/s occurs in the region close to the south pole of the sample. This flow velocity is by a factor of 40 smaller than a widely accepted flow velocity of 0.3 m/s in the electromagnetically levitated samples [30−32]. The damping effect of the static magnetic fields is quite clear. However, both experimental observations [33] and numerical simulation [34] showed that magnetohydrodynamics in an undercooled melt becomes complex once dendritic growth sets in. Another type of forced convection, termed thermoelectric magnetohydrodynamics (TEMHD), develops in the vicinity of a growing dendrite. As illustrated in Fig. 3a, thermoelectric currents exist around the tips of an equiaxed dendrite growing in an undercooled bulk liquid due to

thermal gradients along primary or higher order axes of the dendrite. When a static magnetic field is applied, a Lorentz force will form leading to TEMHD flows around the dendrite. Fig. 3b illustrates TEMHD flow patterns driven by a static magnetic field orientated in the [011] direction relative to the crystallographic orientation of the dendrite. The parallel component of the magnetic field causes the formation of vortices around the [010] tip (parallel to the y axis) and the [001] tip (parallel to the z axis). These vortices can influence the tip kinetics in two ways. The first is a homogenization of the thermal boundary layer local to the tip causing the tip to coarsen and reducing the growth velocity. The second is the formation of a low pressure region at the tip due to a sink-like effect causing bulk fluid become incident promoting tip growth. Additionally, there is a larger scale circulation encompassing both the [010] and [001] tips, which interacts with the bulk when the tips become sufficiently far apart. Local to the primary tip this flow structure acts to bring bulk fluid incident to one side of the tip (promoting growth) and to transport ejected heat ahead of the tip (slowing growth). This mechanism is a consequence of the transverse component of the magnetic field with respect to the growth direction and is highlighted in Fig. 3c, which shows the flow pattern of a single tip under the influence of an orthogonal magnetic field. Interestingly, both parallel and transverse components of the magnetic field can promote or suppress growth. The conditions when one effect dominates over the others are still not well understood. Extensions to the modeling work are currently being developed to explore these mechanisms in more detail and will be presented in a future publication.

We compared dendritic growth velocities under identical undercooling conditions for a quantitative analysis of the effects of the static magnetic fields. First, a series of power laws were fitted to the measured dendritic growth velocities below ΔT_{crit}. Then, the fitted dendritic growth velocities were normalized with respect to with respect to their maxima at given undercoolings and plotted as a function of the magnetic field intensity. As displayed in Fig. 4, the normalized dendritic growth velocities show a U-shaped magnetic field dependence for undercoolings below ΔT = 120 K. Under a low magnetic field ranging between B = 1 T and B = 3 T, the normalized dendritic growth velocities are depressed to a level as low as 15% with respect to their initial values with no magnetic field at ΔT = 20 K. Under higher magnetic fields, the normalized dendritic growth velocities increase progressively with increasing intensity of the magnetic fields. Under the highest magnetic field of B = 6 T, the normalized dendritic growth velocities even exceed their initial levels observed with no magnetic field. The U-shaped dependence is blurred for undercoolings above ΔT = 120 K. This is expected as dendritic growth velocities exceed fluid velocities in this undercooling region.

3.2 Testing of the AG theory using the data of pure nickel

Following the above analysis, we can test the AG theory using the present data. The AG theory [20] predicts the tip selection parameter, σ^*, of a pure substance dendrite growing with convection as

$$\sigma^* = \frac{\sigma_0 \beta^{7/4}}{\left(1 + a_1 \sqrt{\beta} P_g\right)^2 \left[1 + b\left(\alpha(U,R)\beta^{-3/4}\right)^{11/14}\right]}, \quad (1)$$

where $\alpha(U,R) = a(\mathrm{Re})Ud_0/(4RV)$ is the parameter dependent on an incoming flow velocity U with the flow parameter $a(\mathrm{Re}) = \exp(-\mathrm{Re}/2)/E_1(\mathrm{Re}/2)$ and the first exponential integral function $E_1(q) = \int_q^\infty u^{-1}\exp(-u)du$. Re=RUЈ1/ε is the Reynolds number, Ј1 is the density of the liquid, ε is the dynamical viscosity, P_g=VR/(2D_T) is the growth Peclet number, d_0 is the thermocapillary length, R is the dendritic tip radius, V is the dendritic growth velocity, and D_T is the thermal diffusivity of the liquid. The stiffness β = 15Ů4 includes the surface tension anisotropy, Ů4, of the four-fold symmetry. Finally, a_1 å 0.381$\mathring{u}_0$ with $\mathring{u}_0$ the selection constant, and b is the stability constant. The undercooling includes three contributions, namely thermal, ΔT_T, curvature, ΔT_R, and kinetic undercoolings, ΔT_K, and is given by:

$$\Delta T = \Delta T_T + \Delta T_R + \Delta T_K = \frac{\Delta H_f}{C_p} Iv(P_g, P_f) + \frac{2d_0\Delta H_f}{RC_p} + \frac{V}{\mu_k}, \qquad (2)$$

where the ratio of $\Delta H_f/C_p$ is the hypercooling limit (i.e., an undercooling for adiabatic solidification) with ΔH_f the heat of fusion and C_p the heat capacity. μ_k is the interfacial kinetic coefficient, and $Iv(P_g,P_f)$ is the flow-modified Ivantsov function defined by

$$Iv(P_g, P_f) = P_g \exp(P_g + P_f)\int_1^\eta \exp\left[2P_f\int_1^{\eta'}\frac{g(\eta'')}{\sqrt{\eta''}}d\eta'' - (P_f + P_g)\eta'\right]\frac{d\eta'}{\eta'} \qquad (3)$$

with P_f = UR/(2D_T) the flow Peclet number and the hydrodynamic function

$$g(\eta) = \frac{\sqrt{\eta}E_1(\mathrm{Re}\eta/2)}{2E_1(\mathrm{Re}/2)} + \frac{\exp(-\mathrm{Re}/2) - \exp(-\mathrm{Re}\eta/2)}{\sqrt{\eta}\,\mathrm{Re}\,E_1(\mathrm{Re}/2)}. \qquad (4)$$

The dendritic growth velocities of pure nickel can be calculated using Eqs. (1)–(4) if the incoming flow velocity U is known or introduced as a model parameter. A lack of data of absolute thermoelectric power (Seebeck coefficient) of pure nickel at

elevated temperatures makes it difficult to calculate incoming flow velocities under the static magnetic fields. Thus, we treat incoming flow velocities as free parameters in our calculations of dendritic growth velocities. The other parameters used in the calculations are listed in Table 1. The calculated dendritic growth velocities are shown in Fig. 5 and compared with the experimental data. The data measured under the magnetic fields of B = 0 T and B = 6 T can be described by the AG theory assuming an incoming flow velocity of U = 3 m/s and 4 m/s, respectively. Here the assumed flow velocities with no magnetic field are higher than the numerically predicted values of the order of 0.3 m/s for electromagnetically levitated samples [30−32]. As discussed in Section 3.1, the reasons for such higher flow velocities need to be further studied. The data measured under the magnetic fields of B = 1 T to B = 3 T can be described by the AG theory assuming a negligible incoming flow velocity ($U \approx 0$ m/s), and the data measured under the magnetic fields of B = 4 T and B = 5 T can be described by the AG theory assuming an incoming flow velocity of about U = 0.5 m/s. The lower incoming flow velocities under magnetic fields between B = 1 T to B = 5 T are consistent with the prediction of the magnetohydrodynamics simulation on the levitated samples [30]. Note that the measured dendritic growth velocities show a scatter with respect to the calculated values under all magnetic fields. This scatter is not due to experimental errors only, which are less than 10 % of the measured dendritic growth velocities. Rather, it arises largely from a variable angle between the flow direction and the growth direction of the dendrites (see Fig. 3). In the present measurements, the growth direction of the dendrites relies on nucleation sites, which

were not controlled by external trigger as were conducted in previous measurements [10]. Thus, the assumed incoming flow velocities should be viewed as an averaged magnitude of the component of local convective flows in the growth direction of the dendrites. It is implied that the actual flow velocities at the dendritic tips can be higher or lower than the assumed values. Apart from this scatter, the calculated dendritic growth velocities using the AG theory agree in general with the present experimental data. Finally, we note that even though relatively high flow velocities are assumed in our calculations (U is up to 4 m/s as is accepted in Fig. 5), the growth Peclet number lies in the range of accepted values by the AG theory [19, 20] as is shown in Fig. 6. These values of growth Peclet numbers are fully consistent with those obtained in dendritic growth of pure succinonitrile under microgravity condition for low flow velocities (see Section 3.3 and Fig. 7).

3.3 Testing of the AG theory using the data of pure succinonitrile

The AG theory predicts that dendritic tip radii are also sensitive to melt convection at low undercoolings. A complete test of the AG theory should include a comparison with the measured dendritic tip radii. Due to the opaqueness of the nickel melt, it was not possible to measure dendritic tip radii in the present experiment. However, we may use literature data of dendritic growth kinetics measured in pure succinonitrile under normal gravity and microgravity conditions [13] to achieve this goal. We assume that the fluid flow in undercooled melts of pure succinonitrile is caused by natural convection only and that the flow at the dendritic tip is not parallel to the growth direction, but at angle of about 66 degrees. Under such assumptions, we

calculated dendritic growth velocities and dendritic tip radii of pure succinonitrile under normal gravity and microgravity conditions using the parameters listed in Table 1. As shown in Fig. 7a, the calculated dendritic growth velocities under normal gravity condition agree well with the experimental data measured under the same condition over the whole undercooling regime. Similarly, the calculated dendritic growth velocities under a 0.1 % gravity condition agree well with the experimental data measured under the microgravity condition. More importantly, the calculated dendritic tip radii under both gravity conditions show a good agreement with the experimental data over a wide undercooling regime (Fig. 7b). A minor discrepancy is observed for the dendritic tip radii for undercoolings below $\Delta T = 0.1$ K under the microgravity condition. The calculated dendritic tip radii are slightly larger than the measured dendritic tip radii. This discrepancy, however, can be understood if one accepts an enlarged error of about 20% in consideration of difficulties encountered in optical measurements and a non-ideal growth environment[2] [13]. We also compared the calculated growth Peclet numbers with those determined under different gravity conditions. As shown in Fig. 7c, the calculated growth Peclet numbers agree well with the experimentally determined values in the high undercooling region, but show positive deviations in the low undercooling region. We attribute those deviations again to underestimated errors of the measured dendritic tip radii at low undercoolings. The experimentally determined growth Peclet numbers represent a product of two

[2] The size of the growth chamber in one dimension becomes comparable to the thermal diffusion length of the dendrites growing at high undercoolings.

independently measured quantities, dendritic growth velocities and dendritic tip radii. In this sense, the AG theory provides a self-consistent description of the dendritic growth kinetics of pure succinonitrile under normal gravity and microgravity conditions.

3.4 Comparison of the AG theory with phase field modeling

We now compare the AG theory with phase field modeling of three-dimensional dendritic growth. First, dendritic growth at high growth Peclet numbers is considered. Karma and Rappel [23] calculated tip selection parameters as a function of surface tension anisotropy of growing dendrites at a dimensionless undercooling of $\Delta TC_p/\Delta H_f$ = 0.45 (ΔT = 8.096 K) using the phase field method. By fitting an exponential law to their data, we obtain a tip selection parameter of σ^* = 0.01515 for pure succinonitrile assuming a surface tension anisotropy of ε_4 = 0.0055 [13]. This tip selection parameter is close to a value of σ^* = 0.01662 predicted by the AG theory. The difference between them is about 10%. This small difference highlights a good agreement between the AG theory and the phase field modeling. At low growth Peclet numbers, the AG theory predicts a tip selection parameter of σ^* = 0.01852. This value is very close to the experimentally determined values of σ^* = 0.0208 and σ^* = 0.0195 under normal gravity and microgravity conditions [11−13], respectively. At this point, the AG theory bridges the discrepancy between the phase field modeling and the experimental observations. For pure nickel, it has a surface tension anisotropy of ε_4 = 0.018 [37]. The phase field modeling by Karma and Rappel [23] predicted a tip selection parameter of σ^* = 0.064 at a dimensionless undercooling of $\Delta TC_p/\Delta H_f$ =

0.45 (ΔT = 188 K). However, our calculations using the AG theory predicted a tip selection parameter of σ^* = 0.00876 at such a high undercooling (subtracting a kinetic undercooling of ΔT_k = 33 K). This value is about a factor of 7 smaller than the value given by the phase field modeling. Such a large discrepancy in the estimation of the selection parameter can be attributed to a pronounced effect of atomistic kinetics. As addressed elsewhere [37,40,41], the effect of atomistic kinetics may play an essential role in dendrite growth at high undercoolings due to a transition from a surface tension anisotropy-controlled growth behavior to the interfacial kinetic anisotropy-controlled growth behavior. Therefore, for high undercoolings, consistency with analytical and numerical estimations should be made by taking into account both surface tension and atomistic kinetics effects. This will be a goal of future work.

4. Conclusions

The dendritic growth velocities in the undercooled melt of pure nickel have been measured under static magnetic fields up to B = 6 T. The magnetic fields ranging between B = 1 T and B = 5 T cause a deep depression of the dendritic growth velocities at low undercoolings (ΔT < 120 K), whereas the magnetic field of B = 6 T brings about a recovery of the dendritic growth velocities. Numerical modeling has revealed that competing TEMHD flows are formed around dendritic tips and are responsible for the depression and recovery of the dendritic growth velocities. The measured data of pure nickel has been explained using the AG theory in terms of magnetic field-tuned flow velocities. The literature data of dendritic growth velocities

and dendritic tip radii of pure succinonitrile measured under normal gravity and microgravity conditions can also be explained using the AG theory. Such capabilities have demonstrated that the AG theory is able to provide a realistic description of dendritic growth of pure substances with convection. In contrast to an agreement on the tip selection parameter in dendritic growth of pure succinonitrile at high growth Peclet numbers, the AG theory predicts a much smaller tip selection parameter for dendritic growth of pure nickel than that predicted by the phase field modeling. This discrepancy has been attributed to a kinetic transition from the surface tension anisotropy-controlled growth to the interfacial kinetic anisotropy-controlled growth. Efforts will be made to solve this discrepancy.

Acknowledgments

The authors thank Profs. D. M. Herlach, D. Holland-Moritz and G. Wilde for helpful discussion of crystal nucleation and dendritic growth in undercooled melts. The authors thank J. Y. Cai, J. Liu and X. W. Zhao for assistance in experimental work. The authors also thank Drs. J. Gegner, C. Karrasch and S. Cai for providing computer programs for image and data analyses. J. Gao acknowledges support by the National Natural Science Foundation of China (51071043 and 51211130113), Fundamental Research Funds for Central Universities (N09050901 and N130509001), and the Overseas Expert Program of the International Office of Northeastern University. A. Kao and P. Kericleous acknowledge support by the International Exchanges Scheme of the Royal Society of the United Kingdom. D. V. Alexandrov acknowledges support

from the Ministry of Education and Science of the Russian Federation (Project No. 315) and from the Government of the Russian Federation under the contract No. 02.A03.21.0006 (act 211). P. K. Galenko acknowledges support by German Research Foundation (DFG Project RE 1261/8-2) and Russian Foundation for Basic Research (RFBR Project No. 14-29-10282).

List of references

[1] G.P. Ivantsov, Temperature field around spherical, cylindrical and needle-shaped crystals which grow in supercooled melt, Dokl. Akad. Nauk SSSR 58 (1947) 567ï 569.

[2] J.S. Langer, H. Müller-Krumbhaar, Theory of dendritic growth–III. effects of surface tension, Acta Metall. 26 (1978) 1697ï 1708.

[3] J.J. Hoyt, M. Asta, A. Karma, Atomistic and continuum modeling of dendritic solidification, Mater. Sci. Eng. R 41 (2003) 121ï 163.

[4] J. Lipton, W. Kurz, R. Trivedi, Rapid dendrite growth in undercooled alloys, Acta Metall. 35 (1987) 957ï 964.

[5] R. Trivedi, J. Lipton, W. Kurz, Effect of growth rate dependent partition coefficient on the dendritic growth in undercooled melts, Acta Metall. 35 (1987) 965ï 970.

[6] W. Boettinger, S. Coriell, R. Trivedi, Application of dendritic growth theory to the interpretation of rapid solidification microstructures, in: R. Mehrabian, P.A. Parrish (Eds.), Rapid Solidification Processing: Principles and Technologies IV, Claitorôs Publishing Division, Baton Rouge, 1988, pp.13ï 25.

[7] R. Willnecker, D.M. Herlach, B. Feuerbacher, Evidence of nonequilibrium processes in rapid solidification of undercooled metals, Phys. Rev. Lett. 62 (1989) 2707ï 2710.

[8] K. Eckler, R.F. Cochrane, D.M. Herlach, B. Feuerbacher, M. Jurisch, Evidence for a transition from diffusion-controlled to thermally controlled solidification in metallic

alloys, Phys. Rev. B 45 (1992) 5019ï 5022.

[9] C.B. Arnold, M.J. Aziz, M. Schwarz, D.M. Herlach, Parameter-free test of alloy dendrite-growth theory, Phys. Rev. B 59 (1999) 334ï 343.

[10] O. Funke, G. Phanikumar, P.K. Galenko, L. Chernova, S. Reutzel, M. Kolbe, D.M. Herlach, Dendrite growth velocity in levitated undercooled nickel melts, J. Cryst. Growth 297 (2006) 211ï 222.

[11] S.-C. Huang, M.E. Glicksman, Overview 12: fundamentals of dendritic solidification − I. steady-state tip growth, Acta Metall. 29 (1985) 701ï 715.

[12] M.E. Glicksman, M.B. Koss, E.A. Winsa, Dendritic growth velocities in microgravity, Phys. Rev. Lett. 73 (1994) 573ï 576.

[13] M.B. Koss, J.C. LaCombe, L.A. Tennenhouse, M.E. Glicksman, E.A. Winsa, Dendritic growth tip velocities and radii of curvature in microgravity, Metall. Mater. Trans. A 30 (1999) 3177ï 3190.

[14] X. Tong, C. Beckermann, A. Karma, Q. Li, Phase-field simulations of dendritic crystal growth in a forced flow, Phys. Rev. E 63 (2001) 061601.

[15] J.-H. Jeong, J.A. Dantzig, N. Goldenfeld, Dendritic growth with fluid flow in pure materials, Metall. Mater. Trans. A 34 (2003) 459ï 466.

[16] Y. Lu, C. Beckermann, J.C. Ramirez, Three-dimensional phase-field simulations of the effect of convection on free dendritic growth, J. Cryst. Growth 280 (2005) 320ï 334.

[17] B. Nestler, D. Danilov, P.K. Galenko, Crystal growth of pure substances: phase-field simulations in comparison with analytical and experimental results, J.

Comput. Phys. 207 (2005) 221ï 239.

[18] Ph. Boussiou, P. Pelce, Effect of a forced flow on dendritic growth, Phys. Rev. A 40 (1989) 6673ï 6680.

[19] D.V. Alexandrov, P.K. Galenko, Selection criterion of stable dendritic growth at arbitrary Peclet numbers with convection, Phys. Rev. E 87 (2013) 062403.

[20] D.V. Alexandrov, P.K. Galenko, Dendrite growth under forced convection: analysis methods and experimental tests, Physics-Uspekhi 57 (2014) 771ï 786.

[21] S. Binder, P.K. Galenko, D.M. Herlach, The effect of fluid flow on the solidification of Ni_2B from the undercooled melt, J. Appl. Phys. 115 (2014) 053511.

[22] J.-H. Jeong, N. Goldenfeld, J.A. Dantzig, Phase field model for three-dimensional dendritic growth with fluid flow, Phys. Rev. E 64 (2001) 041602.

[23] A. Karma, W.-J. Rappel, Numerical simulation of three-dimensional dendritic growth, Phys. Rev. Lett. 77 (1998) 4050ï 4053.

[24] S. Binder, Undercooling and solidification of tetragonal Ni_2B under different convective flow conditions, PhD Thesis of Ruhr-University Bochum, Bochum, 2010.

[25] K. Eckler, R.F. Cochrane, D.M. Herlach, B. Feuerbacher, Non-equilibrium solidification in undercooled Ni-B alloys, Mater. Sci. Eng. A 133 (1991) 702ï 705.

[26] S.E. Battersby, R.F. Cochrane, A.M. Mullis, Microstructural evolution and growth velocity-undercooling relationships in the systems Cu, Cu-O and Cu-Sn at high undercooling, J. Mater. Sci. 35 (2000) 1365ï 1373.

[27] P.K. Galenko, D.A. Danilov, Local non-equilibrium effect on rapid dendritic growth in a binary alloy melt, Phys. Lett. A 235 (1997) 271ï 280.

[28] J. Gao, Z.N. Zhang, Y.J. Zhang, Measurements of dendritic growth velocities in undercooled melts of pure nickel under static magnetic fields, in: R. Hyers, V. Bojarevis, J. Downey, H. Henein, D. Matson, A. Seidel, D. Voss, M. San Soucie (Eds.), Proceedings of a Symposium on Materials Research in Microgravity 2012 Held at the 141st TMS Annual Meeting and Exhibition, Orlando, USA, March 11-15, 2012, NASA/CP-2012-217466, pp. 72ï 79.

[29] H. Yasuda, I. Ohnaka, Y. Ninomiya, R. Ishii, S. Fujita, K. Kishio, Levitation of metallic melt by using the simultaneous imposition of the alternating and the static magnetic fields, J. Cryst. Growth 260 (2004) 475ï 485.

[30] V. Bojarevics, K. Pericleous, Modeling electromagnetically levitated liquid droplet oscillations, ISIJ Inter. 43 (2003) 890ï 898.

[31] R.W. Hyers, Fluid flow effects in levitated droplets, Meas. Sci. Technol. 16 (2005) 391ï 401.

[32] J.H. Lee, D.M. Matson, S. Binder, M. Kolbe, D. Herlach, R.W. Hyers, Magnetohydrodynamic modeling and experimental validation of convection inside electromagnetically levitated Co-Cu droplets, Metall. Mater. Trans. B 45 (2014) 1018ï 1023.

[33] X. Li, Y. Fautrelle, Z. Ren, Influence of thermoelectric effects on the solid-liquid interface shape and cellular morphology in the mushy zone during the directional solidification of Al-Cu alloys under a magnetic field, Acta Mater. 55 (2007) 3803ï 3813.

[34] A. Kao, G. Djambazov, K. Pericleous, V. Voller, Thermoelectric MHD in

dendritic solidification, Magnetohydrodynamics 45 (2009) 267ï 277.

[35] K. C. Mills, B.J. Monaghan, B.J. Keene, Thermal conductivities of molten metals: part 1 pure metals, Inter. Mater. Rev. 41 (1996) 209ï 242.

[36] T. Iida, I.L. Guthrie, The Physical Properties of Liquid Metals, Oxford University Press Inc., New York, 1988.

[37] J. Bragard, A. Karma, Y.H. Lee, M. Plapp, Linking phase-field and atomistic simulations to model dendritic solidification in highly undercooled melts, Inter. Sci. 10 (2002) 121ï 136.

[38] J. Monk, Y. Yang, M.I. Mendelev, M. Asta, J.J. Hoyt, D.Y. Sun, Determination of the crystal-melt interface kinetic coefficient from molecular dynamics simulations, Modeling Simul. Mater. Sci. Eng. 18 (2010) 015004.

[39] J. Bokeloh, R.E. Rozas, J. Horbach, G. Wilde, Nucleation barriers for the liquid-to-crystal transition in Ni: experiment and simulation, Phys. Rev. Lett. 107 (2011) 145701.

[40] E.A. Brener, Effects of surface energy and kinetics on the growth of needle-like dendrites, J. Cryst. Growth 99 (1990) 165ï 170.

[41] D.V. Alexandrov, P.K. Galenko, Thermo-solutal and kinetic regimes of an anisotropic dendrite growing under forced convective flow, Phys. Chem. Chem. Phys. 17 (2015) 19149ï 19161.

List of figure captions

Fig. 1 Measured dendritic growth velocities of pure nickel as a function of undercooling under static magnetic fields between B = 0 T and B = 6 T. The relative errors of individual measurements are less than 10%. Error bars of data points are not shown for clarity. Previous data measured by Funke et al. [10] in electromagnetically levitated samples of higher purity (99.999%) is also shown for comparison.

Fig. 2 Illustration of numerically simulated temperature and fluid velocity in an inductively melted Ni sample of a spherical geometry under a static magnetic field of B = 6 T. The r axis shows the distance from the sample center in the radial direction of the spherical sample.

Fig. 3 Illustration of (a) thermoelectric currents, (b) and (c) TEMHD flows around an equiaxed dendrite growing from an undercooled melt. Note in (a) that thermoelectric currents circulate from cool tips to their warm roots. In (b), the parallel component of a tilted magnetic field causes the formation of vortices around the tips in the y and z directions. In (c), the transverse component of the static magnetic field causes the formation of an incident flow at a local tip. More details are described in the text.

Fig. 4 Normalized dendritic growth velocities of pure nickel versus static magnetic fields under identical undercooling conditions. The curves show a guide to the eye.

Fig. 5 Calculated dendritic growth velocities of pure nickel under static magnetic fields of B = 0 T, 2 T, 4 T and 6 T using the AG theory. The incoming flow velocities U are unknown and chosen for a least square fit to the measured data.

Fig. 6 Calculated growth Peclet number of pure nickel as a function of undercooling for different flow velocities.

Fig. 7 Comparison of measured and calculated dendritic growth velocities (*a*), dendritic tip radii (*b*) and growth Peclet numbers (*c*) of pure succinonitrile under normal gravity and microgravity (μg) conditions. The measured data is taken from Ref. [13]. It is assumed that flow is caused by natural convection only and has an angle of about 66 degrees with respect to the growing direction of the dendritic tip.

List of tables

Table 1 Materials parameters used in the calculations of dendritic growth velocities

Parameter	Nickel	Succinonitrile	Reference
Thermal diffusivity, D_T (m^2/s)	1.2×10^{-5}	1.13×10^{-7}	[13, 35]
Hypercooling limit, $\Delta H_f/C_p$ (K)	418	23.13	[13, 36]
Thermocapillary length, d_0 (m)	$4.92\times10^{-10*}$	2.821×10^{-9}	[13]
Liquid density, ρ_l ($kg\cdot m^{-3}$)	7900	982	[13, 36]
Dynamic viscosity, μ ($Pa\cdot s$)	5.64×10^{-3}	2.64×10^{-3}	[13, 36]
Surface tension anisotropy, ε_4 (-)	0.018	0.0055	[13, 37]
Kinetic coefficient, μ_k ($m\cdot s^{-1}\cdot K^{-1}$)	—	0.71	[38]
Selection constant, σ_0 (-)	0.089	1.46	Present work
Stability constant, b (-)	0.1	0.1	[20]

* The thermocapillary length of pure nickel is calculated using a solid-liquid interfacial energy of 0.275 J/m^2 given in Ref. [39].

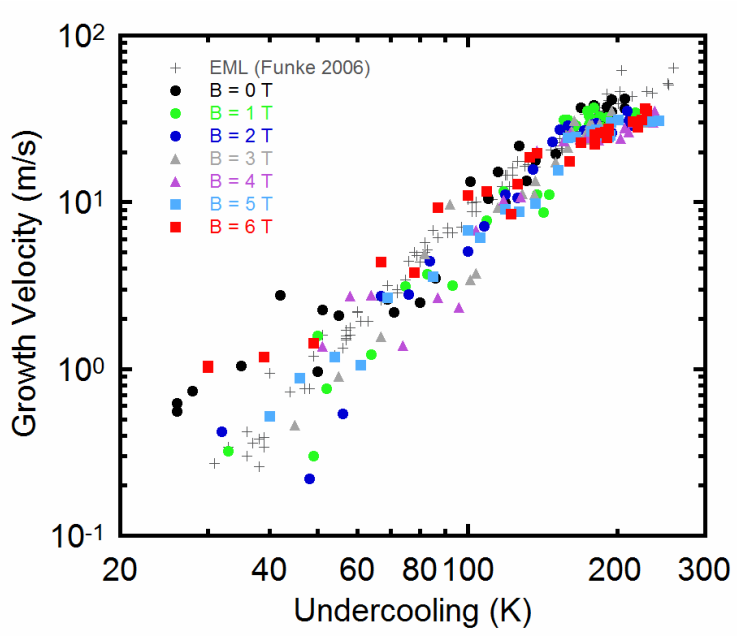
EML (Funke 2006)
B = 0 T
B = 1 T
B = 2 T
B = 3 T
B = 4 T
B = 5 T
B = 6 T
Growth Velocity (m/s)
Undercooling (K)

Fig. 1

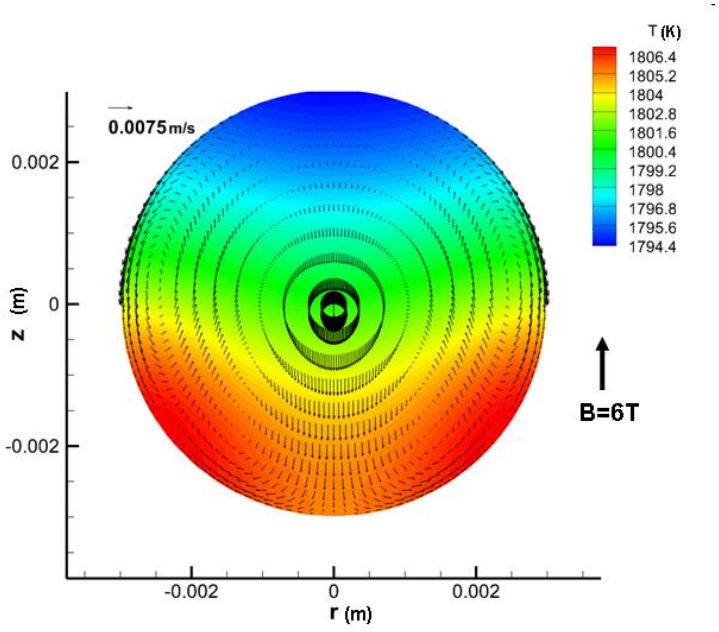
T (K)
1806.4
1805.2
1804
1802.8
1801.6
1800.4
1799.2
1798
1796.8
1795.6
1794.4
0.0075 m/s
B=6T
z (m)
r (m)

Fig. 2

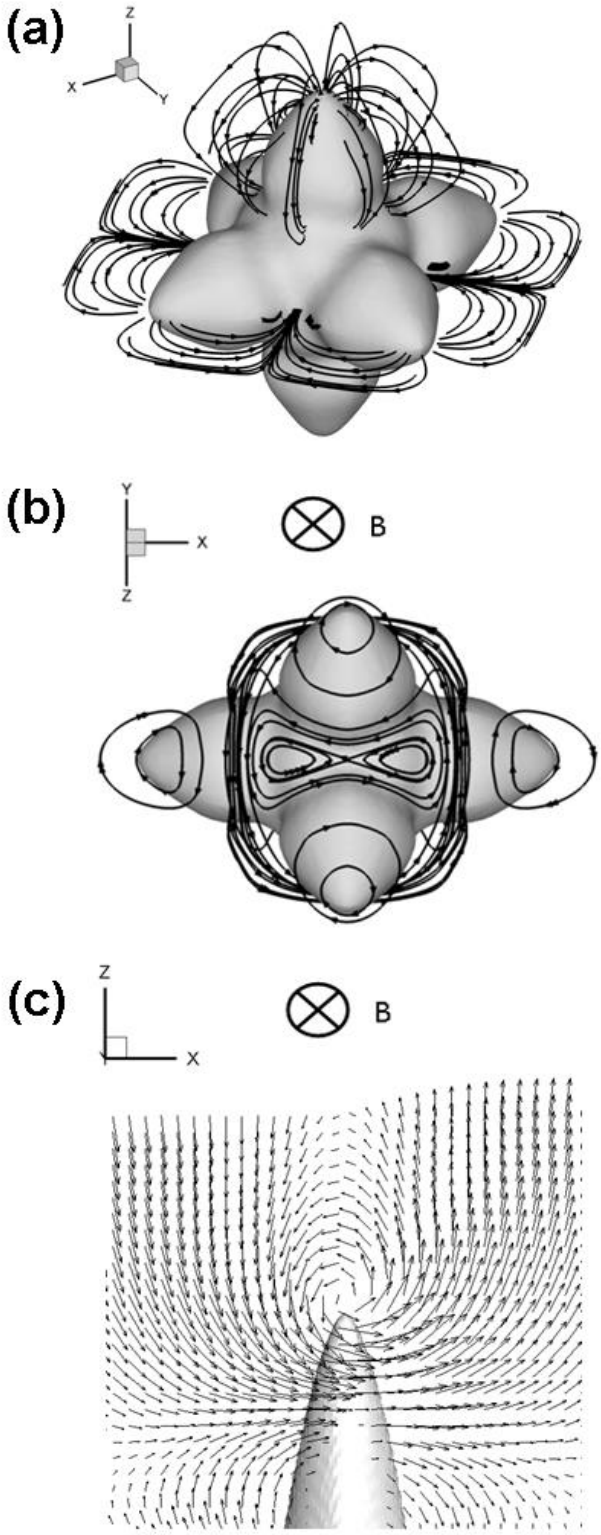

Fig. 3

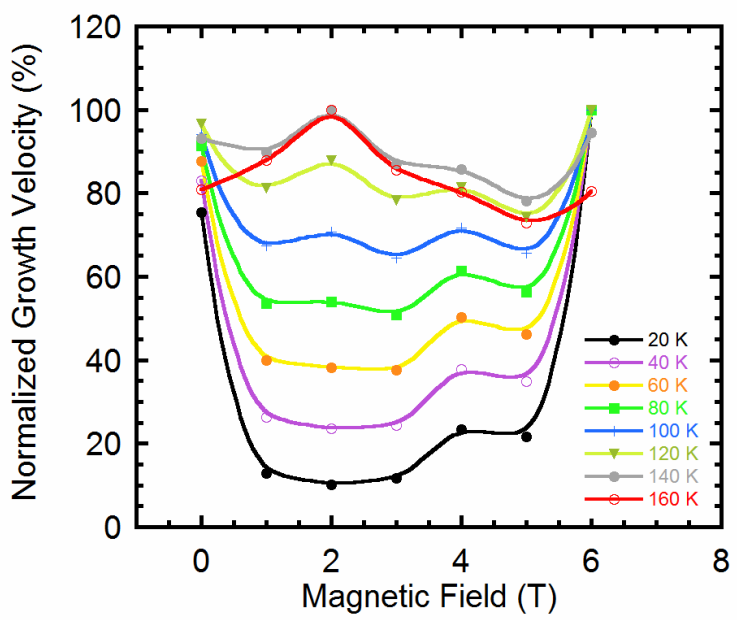
Normalized Growth Velocity (%)
Magnetic Field (T)
20 K
40 K
60 K
80 K
100 K
120 K
140 K
160 K

Fig. 4

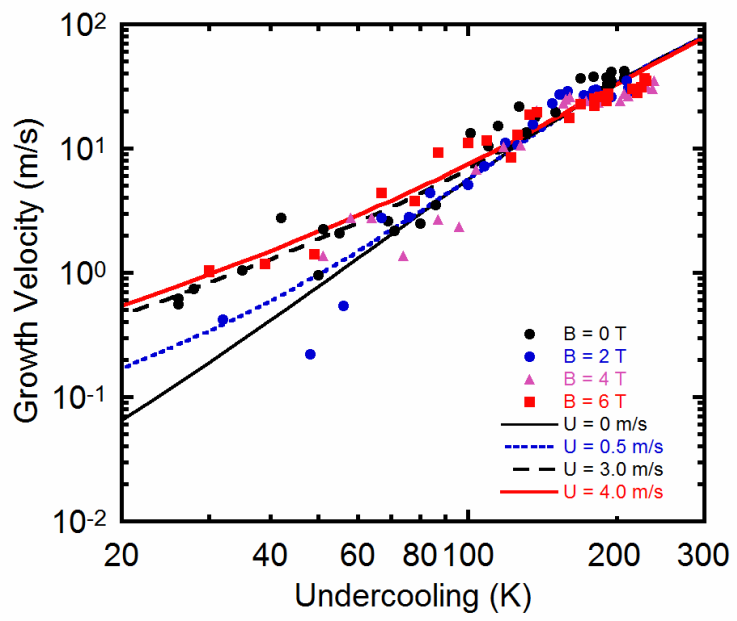
Growth Velocity (m/s)
Undercooling (K)
B = 0 T
B = 2 T
B = 4 T
B = 6 T
U = 0 m/s
U = 0.5 m/s
U = 3.0 m/s
U = 4.0 m/s

Fig. 5

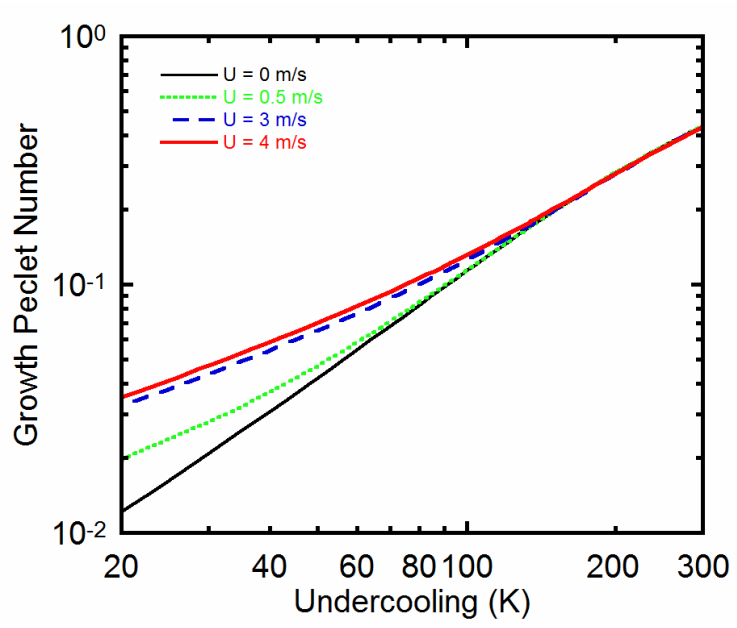
U = 0 m/s
U = 0.5 m/s
U = 3 m/s
U = 4 m/s
Growth Peclet Number
Undercooling (K)

Fig. 6

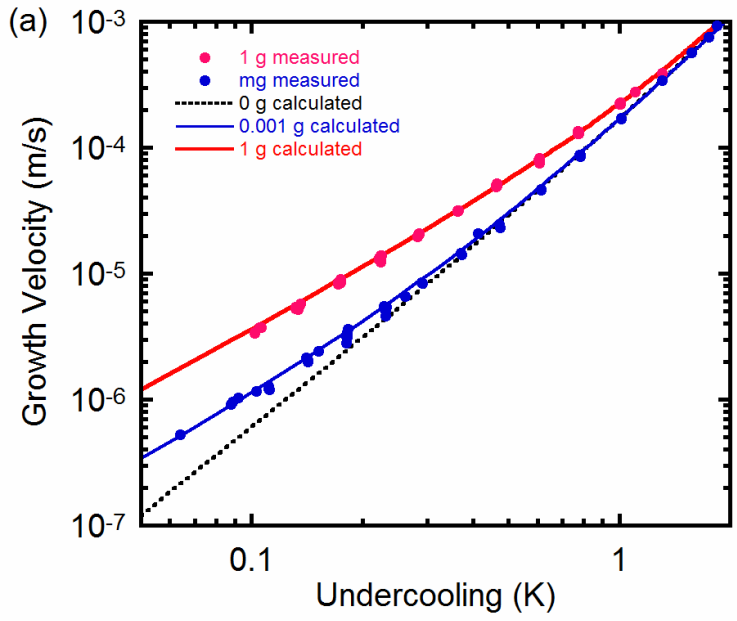
(a)
1 g measured
mg measured
0 g calculated
0.001 g calculated
1 g calculated
Growth Velocity (m/s)
Undercooling (K)

Fig. 7a

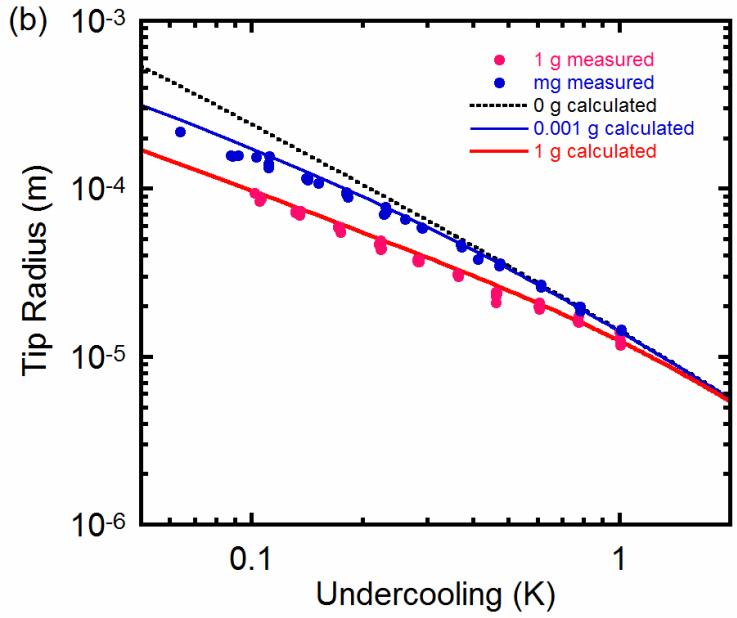
(b)
10-3
10-4
10-5
10-6
Tip Radius (m)
0.1
1
Undercooling (K)
1 g measured
mg measured
0 g calculated
0.001 g calculated
1 g calculated

Fig. 7b

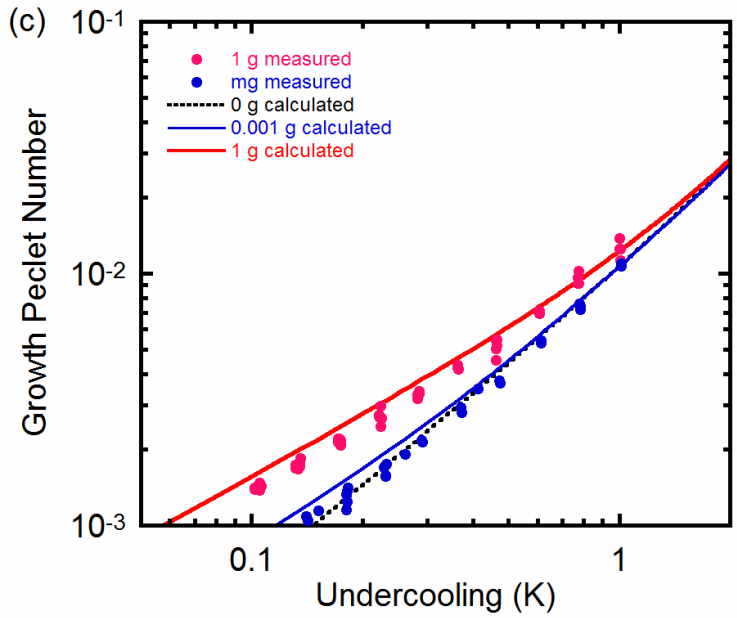
(c)
10-1
10-2
10-3
Growth Peclet Number
0.1
1
Undercooling (K)
1 g measured
mg measured
0 g calculated
0.001 g calculated
1 g calculated

Fig. 7c

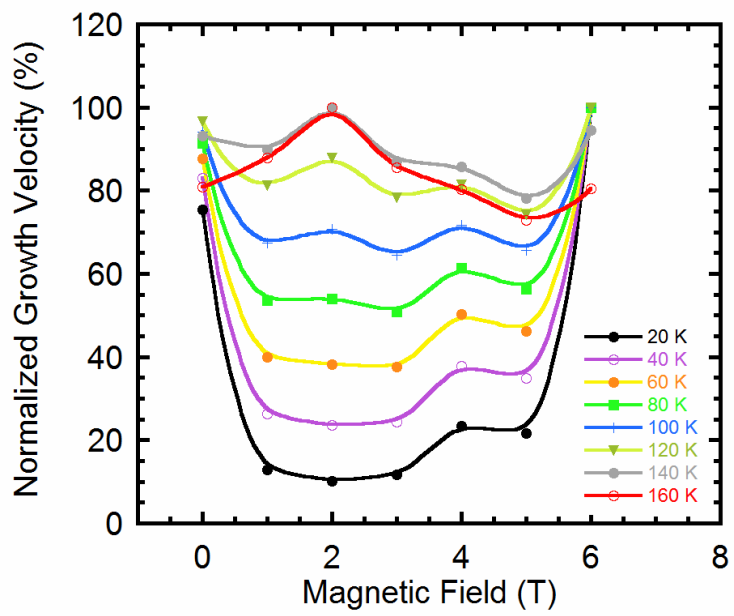

Graphic abstract